JOURNAL OF VIROLOGY, Mar. 2005, p. 3084–3096 Vol. 79, No. 5
0022-538X/05/$08.00+0 doi:10.1128/JVI.79.5.3084–3096.2005

Human Cytomegalovirus Tegument Protein ppUL35 Is Important for Viral Replication and Particle Formation

Karina Schierling,[1] Christopher Buser,[1,2] Thomas Mertens,[1] and Michael Winkler[1]*

Abteilung Virologie, Universitätsklinikum Ulm,[1] and Zentrale Einrichtung Elektronenmikroskopie,[2] Ulm, Germany

Received 23 July 2004/Accepted 12 November 2004

The tegument proteins ppUL35 and ppUL82 (pp71) of human cytomegalovirus (HCMV) physically interact and cooperatively activate the major immediate-early transcription. While an HCMV mutant lacking UL82 displayed a multiplicity of infection (MOI)-dependent growth, the biological significance of ppUL35 has not been addressed so far. We generated a mutant virus with a deletion of the UL35 gene. Using an MOI of 0.1, the progeny virus yield of this mutant was reduced by a factor of 1,000; however, when infected at a low MOI (0.01), the gene was essential. Characterization of the replication cycle showed that the mutant virus had two defects: when virus inoculum was standardized by the amount of viral DNA, a reduced immediate-early gene expression was observed, leading to a strongly delayed expression of lytic genes. A second defect was apparent in the virus assembly, as fewer enveloped particles and no dense bodies were present in cells infected with the mutant virus. However, the particles produced by wild-type and mutant viruses did not show significant ultrastructural differences. These results suggest an important role for ppUL35 in immediate-early gene expression and virus assembly.

Human cytomegalovirus (HCMV) is an exclusively human pathogen causing considerable morbidity and mortality in individuals with immature or compromised immune systems (34). HCMV is classified as a herpesvirus belonging to the *Betaherpesvirinae* subfamily. The genome of HCMV, comprising 235 kbp, is one of the largest genomes of animal viruses, encoding 165 to 190 genes, depending on the method of prediction (12, 30). A substantial part of the coding potential is devoted to virion proteins.

The virion of HCMV is composed of at least 40 proteins and has a tripartite structure, consisting of an envelope, a tegument, and a capsid (16, 43). The tegument is a proteinaceous structure, interspersed between the envelope and the capsid, and is characteristic of herpesviruses. Whereas the envelope and capsid are relatively well defined, characterization of the tegument has lagged behind. Long regarded as an unstructured repository for proteins, the tegument is now thought to have an ordered architecture and multiple functions (27).

At present, about 20 proteins have been localized to the tegument of HCMV, and they have been implicated in virion formation (3, 28), virus transport (41), immunomodulation (8, 10, 17) and transactivation. The first tegument protein which was shown to be involved in the activation of the major immediate-early enhancer-promoter (MIEP) of HCMV was ppUL82 (pp71) (23). Later, another regulatory protein, pUL69, was found in the tegument and was shown to transactivate the MIEP cooperatively with ppUL82 (47, 48). These observations were reproduced and extended, with the HCMV TRS1/IRS1 and UL35 genes added to the list (24, 36). Recently, we were able to show a physical interaction between two of these cooperatively *trans*-activating proteins, ppUL82 and ppUL35 (38). The UL35 gene encodes two proteins, of which the shorter form, ppUL35A, corresponds to the C-terminal part of full-length ppUL35 (24). Both forms can physically interact with ppUL82, but only full-length ppUL35 cooperates with ppUL82 (24, 38).

The biological significance of several genes encoding tegument proteins has been explored using antisense strategies or virus mutants. These studies showed that two abundant tegument proteins, ppUL32 and ppUL99, are essential for virus growth in cell culture (28, 40). Whereas ppUL32 appeared to play a role in the cytoplasmic accumulation of virions, there was an accumulation of tegumented capsids in the cytoplasm of cells infected with mutant viruses lacking ppUL99. Surprisingly, another abundant protein, ppUL83 (pp65), is not essential for growth in cell culture (39). However, since ppUL83 has immunomodulatory functions (8, 17), it likely plays an important role for the infected organism. The deletion of the gene encoding tegument protein pUL47 led to a 100-fold reduction in viral titers, irrespective of whether infection was done at high ($\geq$1) or low ($\leq$0.01) multiplicities of infection (MOIs) (4).

In contrast, deletions of the two regulatory tegument proteins ppUL82 and ppUL69 led to an MOI-dependent growth defect (19). This means that mutant virus can grow to some extent when infections are performed at high MOIs, but the genes appear to be essential after infection at low MOIs. A common denominator of several of these tegument proteins is that they are implicated in regulatory processes during the immediate-early (IE) phase. A direct effect on IE gene expression has been demonstrated for ppUL82 (6). An MOI-dependent growth phenotype was also observed for mutants of ppUL123 (IE1) (14) and those with mutations in the enhancer region (15) and is therefore consistent with a model in which the level of IE gene expression determines the outcome of infection. A role for virion-associated factors is supported by the observation that growth of HCMV lacking the distal part of the enhancer can be augmented by UV-inactivated HCMV

* Corresponding author. Mailing address: Abteilung Virologie, Universitätsklinikum Ulm, Albert Einstein Allee 11, D-89081 Ulm, Germany. Phone: 49 731 5002 3336. Fax: 49 731 5002 3337. E-mail: michael.winkler@medizin.uni-ulm.de

virions (25). Analysis of MCMV with deletion of the enhancer demonstrated that the MOI-dependent growth phenotype is also reflected in a drastically reduced virulence in vivo (15).

Here, we characterized a mutant virus lacking the UL35 gene region. We showed that the deletion of the UL35 gene affects IE gene expression. In addition, we observed an impaired maturation of virus particles leading to reduced numbers of enveloped particles and a lack of dense bodies.

MATERIALS AND METHODS

Oligonucleotides. The following oligonucleotides were obtained from MWG (Ebersberg, Germany), Sigma/ARK (Darmstadt, Germany), or Biomers (Ulm, Germany): CMV-IE-Plus, CGTCCTTGACACGATGGAGTC; CMV-IE-Minus, TCGGGGTTCTCGTTGCAATCC; Aktin4, AGCCATGTACGTAGCCATCCAGGCT; Aktin5, GGATGTCAACGTCACACTTCATGATGG; ETH257, TGAACCTCGAGTCTGTCATCACGGTACACAGA; ETH258, GAAGCTTGGCGGCCGCCAACGGGGTTATGGGGGACGTG; ETH417, TGAACGTCGACGACGACCTACGGGACACGCTGATG; ETH418, GAAGCTTGGCGGCCGCCGAACAGACGGTGCCCATCTTG; UL35-ko3, CGACGTCTCATCTTGAGACAGACACGTAGAAAAAGAGGAAAAACCGCTTACAAGGACGACGACGACAAGTAA; UL35-ko5, TTCTCAAGTTCCGCTCTGGTTTTGGTTTCGTTTTCAAAGGGAGCCCCATCCGTCGTGGAATGCCTTCGAATTC; UL35-kon5, CTGGAGAACAATAAAGCG; UL35-kon3, CTGTGTACTTCGCTAGTC; rv35-5, TTCTCAAGTTCCGCTCTGGTTTTGGTTTCGTTTTCAAAGGGAGCCCCATCATGGCCCAAGGATCGCGAGC; rv35-3, CGACGTCTCATCTTGAGACAGACACGTAGAAAAAGAGGAAAAACCGCTTCGTCGTGGAATGCCTTCGAATTC; UL35kon3, CTGTGTACTTCGCTAGTC; UL35kon5, CTGGAGAACAATAAAGCG.

Plasmid constructions. Plasmid pKD46 contains the phage λ recombination genes Redαβγ under the control of the arabinose-inducible P_{araB} promoter (11). This plasmid also contains the temperature-sensitive origin *oriR101* and grows well at 30°C but not at 37°C. Plasmid pCP20 encodes the FLP recombinase and allows growth at 30°C but not at 43°C due to a pSC101-based temperature-sensitive origin (9). Plasmid pSL-FRT contains the kanamycin resistance gene flanked by FRT sites in vector pSL301 (Amersham Biosciences, Freiburg, Germany) (2). Plasmid pBRep-Cre harbors the Cre recombinase expression cassette from plasmid pMC-Cre and the bovine papillomavirus replication origin (18, 21). Plasmid pSL-FRT-UL35 was constructed by excising the UL35 open reading frame as an Asp718I/XhoI fragment from pcDNA3-UL35 (38) followed by insertion into the Asp718I/SalI sites of pSL-FRT.

Fragments corresponding to the sequences adjacent to UL35 were cloned into vector pBlueKan (38), a modified version of pBluescript KS II, where the ampicillin resistance cassette has been replaced by a kanamycin resistance cassette. Plasmid pBlueKan-UL34 was constructed by PCR amplification using primers ETH257 and ETH258 and subsequent cloning via XhoI/NotI. Similarly, UL36 exon 1 was amplified using primers ETH417 and ETH418 and cloned into pBlueKan via SalI and NotI sites.

Engineering BAC mutants. Recombinant bacterial artificial chromosome (BAC) clones were generated by RecET-based recombination using the RecET homologues of phage λ, Redαβγ (44). For deletion of the UL35 open reading frame, we used HCMV AD169-BAC(pHB15), containing the complete AD169 genome (21), and plasmid pKD46 (11) in *Escherichia coli* strain DH10B. First, the kanamycin gene, flanked by FRT sites, was amplified by PCR with oligonucleotides containing 50 nucleotides of sequence homologous to the region 5′ and 3′ of the UL35 gene (UL35-63/UL35-ko5). The PCR product was then transformed into an *E. coli* strain containing the HCMV AD169-BAC, where the RecET recombination system catalyzed the exchange of the UL35 open reading frame with the resistance marker. Subsequently, we deleted the kanamycin resistance cassette by FLP-mediated recombination between the two FRT sites flanking the resistance marker. By use of this procedure, the UL35 open reading frame was deleted, thus generating *del*UL35-BAC. A single FRT site and an additional EcoRI restriction marker remained as marks of the recombination procedure.

In order to generate a revertant virus, we used plasmid pSL-FRT-UL35. A PCR product containing both UL35 and the FRT-flanked kanamycin marker was generated using oligonucleotides containing sequences homologous to the region 5′ and 3′ of the UL35 gene (rv35-3/rv35-5). This PCR product was recombined into the UL35 region of the *del*UL35-BAC via RecET recombination. Finally, the kanamycin resistance cassette was again deleted by FLP-mediated recombination. Hereby, a revertant BAC, *rev*UL35-BAC, which differs from the wild-type AD169-BAC by a single FRT site and an EcoRI restriction site remaining at the 3′ end of the UL35 open reading frame was generated.

Electrocompetent *E. coli* DH10B (containing the respective BAC and pKD46) for transformation of the PCR products was prepared as described previously (44). PCR fragments for mutagenesis were prepared using primer pair UL35-ko3/UL35-ko5 and template pSL-FRT for generation of the UL35 deletion virus or primer pair rv35-3–rv35-5 and template pSL-FRT-UL35 for the generation of the revertant BAC. Amplification was done using a touchdown protocol, and PCR products were processed as described previously (44). Briefly, PCR products were purified using a PCR purification kit (QIAGEN, Hilden, Germany), digested with DpnI to inactivate template DNA, and ethanol precipitated. Electrocompetent bacteria were transformed with the processed PCR product, plated onto Luria-Bertani (LB) agar plates containing 25 μg of chloramphenicol/ml and 30 μg of kanamycin/ml, and grown overnight at 37°C. Single colonies were analyzed by colony PCR using primers UL35kon3 and UL35kon5, which bound outside the region involved in the recombination. Colonies containing a correct insertion of the PCR cassette were transformed with plasmid pCP20 to remove the kanamycin resistance marker and grown overnight at 30°C in LB liquid medium containing 25 μg of chloramphenicol/ml and 50 μg of ampicillin/ml. A small aliquot of this culture was then plated on LB agar plates containing 25 μg of chloramphenicol/ml and grown overnight at 43°C to select against plasmid pCP20. Single colonies were analyzed for removal of the kanamycin resistance marker by colony PCR using primers UL35kon3 and UL35kon5.

Southern blotting. Digested BAC DNA was separated on 0.6% agarose gels and transferred to Biodyne B nylon membranes (Pall, Dreieich, Germany). Double-stranded DNA probes were radioactively labeled using the Ready-To-Go kit (Amersham Biosciences) and [α-^{32}P]dCTP. Radioactive hybridizations were performed with a hybridization incubator (Robbins Scientific, Sunnyvale, Calif.) essentially as described previously (46). Briefly, filters were prehybridized for at least 4 h at 42°C in a prehybridization solution containing 50% formamide, 5× SSC (1× SSC is 0.15 M NaCl plus 0.015 M sodium citrate), 50 mM sodium phosphate (pH 6.5), 5× Denhardt's solution, and 1 mg of yeast RNA (Fluka, Taufkirchen, Germany)/ml. Hybridizations were performed for at least 24 h in a hybridization solution containing 50% formamide, 5× SSC, 20 mM sodium phosphate (pH 6.5), 5× Denhardt's solution, and 500 μg of yeast RNA/ml. Thereafter, filters were washed several times with buffer containing 20 mM sodium phosphate–0.1% sodium dodecyl sulfate (SDS) and decreasing concentrations of SSC. For reprobing of the filters, the radioactive probe was removed by two incubations in 0.1% SDS at 95°C for 30 min.

To analyze viral replication, human fibroblasts were seeded in six-well plates at 2.5×10^5 cells/well. One day later, the cells were infected for 4 h with mutant virus (RV*del*UL35) at an MOI of 0.1 or with wild-type virus (RV*wt*AD169) at an MOI of 0.1 or 1. For harvesting, cells were trypsinized and pelleted, and the cell pellet was resuspended in 100 μl of phosphate-buffered saline (PBS). To digest proteins, 3 μl of proteinase K (10 mg/ml) was added, and the samples were incubated for 1 h at 56°C. After inactivation at 95°C (10 min), probes were denatured by the addition of 40 μl of 2 N NaOH and transferred to a nylon membrane by use of a slot blot chamber (Schleicher & Schuell, Keene, N.H.). Viral DNA was detected by hybridization with a radioactively labeled probe for UL36 as described above. For phosphorimager quantitation of the signals, the FLA3000 scanner (Fuji, Tokyo, Japan) and AIDA 2D quantification software (Raytest, Straubenhardt, Germany) were used.

Cell lines and culture. Human foreskin fibroblasts (HFF) were maintained in minimal essential medium (Gibco/BRL, Eggenstein, Germany) supplemented with 10% fetal calf serum, 2 mM L-glutamine (Biochrom AG, Berlin, Germany), 100 U of penicillin and 100 μg of streptomycin (Gibco/BRL), each per ml, and 1× nonessential amino acids (Biochrom AG, Berlin, Germany).

Antibodies. Monoclonal antibodies directed against ppUL69 (69-66), ppUL82 (CMV355), ppUL83 (28–77), gpUL55 (gB) (27–287), and ppUL99 (41-18) have been described previously (7, 33, 45). Monoclonal antibodies E13 (35), CCH2, and Ab-1 directed against HCMV IE proteins, pUL44, and cellular vimentin, respectively, were purchased from Argene (Varilhes, France), DAKO (Hamburg, Germany), and Oncogene Research Products (Boston, Mass.). Rabbit antiserum directed against pUL35 was kindly provided by B. Biegalke (24).

Virus reconstitution, titration, and growth curves. For virus reconstitution, HCMV-BAC DNA was isolated from *E. coli* by using a Nucleobond AX kit (Macherey & Nagel, Düren, Germany). For electroporation of HCMV AD169-BAC DNA, HFF were trypsinized, washed two times with medium, and resuspended at a density of 10^7/ml. The transfection mixture, consisting of about 5 μg of BAC DNA, 5 μg of pCMV71 (23), and 0.5 μg of pBRep-Cre (21), was mixed with 400 μl of cell suspension. Electroporation was performed with an Easyject Optima electroporation device (Peqlab, Erlangen, Germany) at 280 V and 1,500 μF. Cells were immediately mixed with fresh medium and transferred to 75-cm^2

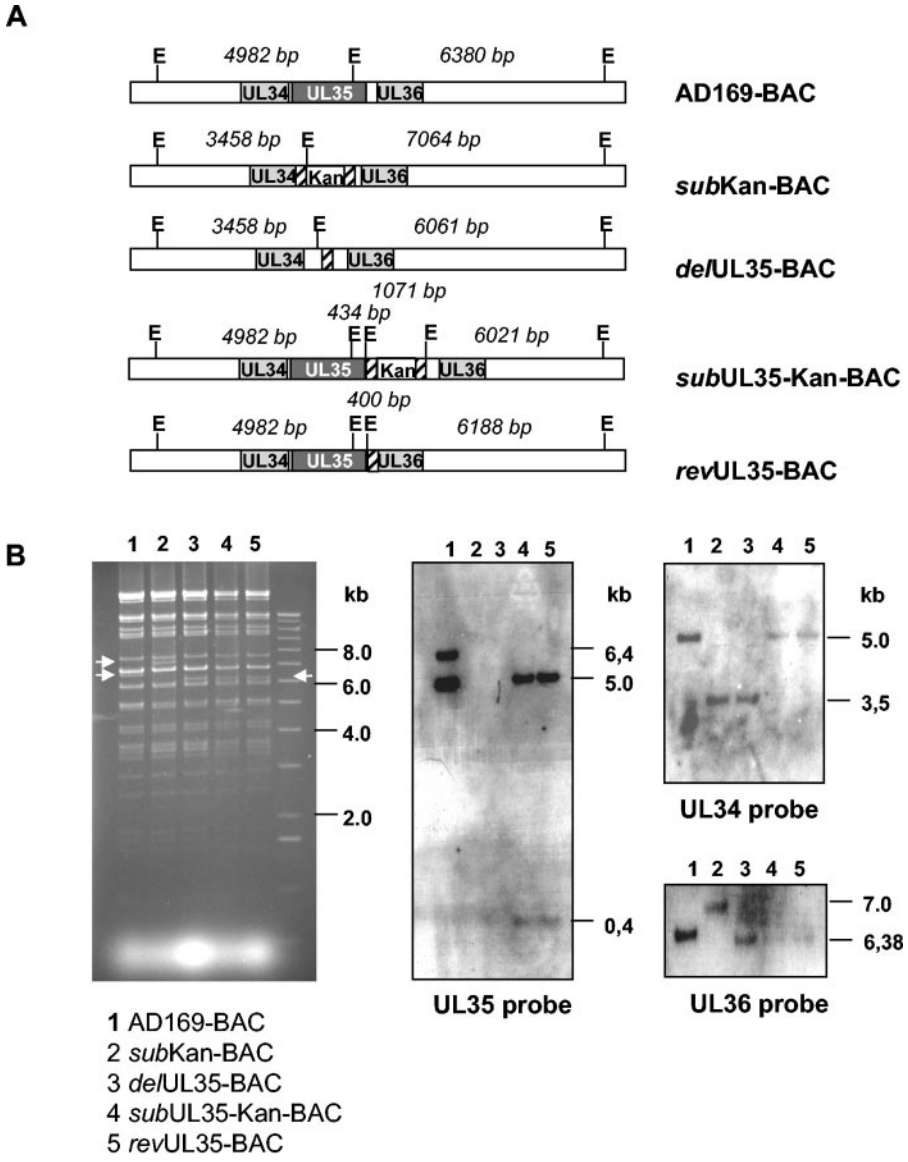

FIG. 1. Construction of the *del*UL35-BAC. (A) Schematic representation of the UL35 gene region in the genomes of HCMV AD169-BAC, *del*UL35-BAC (mutant), and *rev*UL35-BAC (revertant) and intermediate constructs containing the kanamycin resistance cassette (*sub*Kan-BAC and *sub*UL35-Kan-BAC). Open reading frames are depicted as boxes with the respective names of the genes. Cross-hatched boxes indicate the positions of the FRT sites. EcoRI restriction sites and sizes of the resulting DNA fragments are indicated. (B) Restriction analysis of the BAC genomes shown in panel A. BAC DNA was digested with EcoRI and separated by agarose gel electrophoresis. Changes in the sizes of restriction fragments are indicated by arrows (left panel). Results of Southern blot analysis of this gel are shown in the middle and right panels. DNA fragments were transferred to nitrocellulose membranes and analyzed with ^{32}P-labeled probes recognizing UL34, UL35, and UL36. DNA size markers are shown on the right.

flasks. After overnight incubation, the cells were washed and supplemented with fresh medium. When most cells showed a cytopathic effect, they were trypsinized, mixed with about 2×10^7 HFF, and seeded in 175-cm^2 flasks. Virus supernatant was harvested when a confluent cytopathic effect was apparent. Viral particles were pelleted by ultracentrifugation in a Beckman (Munich, Germany) SW28 rotor at 22,000 rpm for 1 h at 4°C. Pellets were resuspended in a 1:1 mixture of medium–0.2 M sucrose phosphate, and aliquots were stored at −80°C (22). The recombinant viruses (RV) recovered from AD169-BAC, *del*UL35-BAC, and *rev*UL35-BAC were named RV*wt*AD169, RV*del*UL35, and RV*rev*AD169, respectively.

For quantitation of DNA in viral particles, a total of 10^5 PFU was pelleted in an Eppendorf tube by centrifugation at 23,000 × *g* at 4°C for 2 h. The pellet was resuspended in 50 μl of H_2O and 50 μl of lysis buffer B (60 mM Tris-HCl [pH 8.3], 100 mM KCl, 5 mM $MgCl_2$, 0.2 mg of gelatin, 0.9% Tween 20). Proteins were degraded by the addition of 3 μl of proteinase K (10 mg/ml) and incubation at 56°C for 1 h. After inactivation of proteinase K at 95°C for 10 min, insoluble material was pelleted by centrifugation (5 min at 16,000 × *g*), and the supernatant was used for the determination of the amount of DNA.

Entry of viral DNA into cells. HFF were seeded into six-well plates at a density of 2.5×10^5 cells per well. The next day, the cells were infected at an MOI of 0.1 PFU/cell. At 6 h postinfection (hpi), the cells were trypsinized and transferred to an Eppendorf tube. DNA was isolated essentially as described previously (42), with some modifications. The cell pellet was resuspended in 250 μl of buffer C1 (40 mM Tris-HCl, 20 mM $MgCl_2$, 1.28 M sucrose, 4% Triton X-100) and incubated on ice for 10 min to permeabilize the cells but to leave the nuclei intact. The nuclei were collected by centrifugation at 1,300 × *g* and 4°C for 15 min, and the pellet was resuspended in 50 μl of buffer C2 (10 mM Tris-HCl [pH 7.5], 2 mM $MgCl_2$, 10% sucrose). After the addition of 50 μl of 2× nuclease

buffer {40 mM PIPES [piperazine-N,N′-bis(2-ethanesulfonic acid)] [pH 7.0], 7% sucrose, 20 mM NaCl, 2 mM $CaCl_2$, 10 mM β-mercaptoethanol, 0.2 mM PMSF [phenylmethylsulfonyl fluoride]}, the samples were incubated for 30 min at 37°C. After the addition of 6 μl of 0.2 M EDTA and 400 μl of digestion buffer (10 mM Tris-HCl [pH 8.0], 100 mM NaCl, 25 mM EDTA, 0.5% SDS, 0.1 mg of proteinase K/ml), the samples were incubated overnight at 50°C. After phenol-chloroform extraction and ethanol precipitation, the DNA pellet was dissolved in 100 μl of H_2O. For quantitation, 10-fold dilutions were prepared and used for PCR amplification with primer pair CMV-IE-Plus–CMV-IE-Minus or Aktin4-Aktin5.

Immunoblotting. Cell extracts were separated on 10 or 12% polyacrylamide gels and blotted onto polyvinylidene difluoride membranes (Bio-Rad, Munich, Germany) by semidry electrophoresis using the Transblot SD apparatus (Bio-Rad). To avoid nonspecific antibody binding, filters were blocked for 1 h in 3% skim milk powder–PBS. For detection of specific proteins, filters were incubated with primary antibody at room temperature for 1 h. Rabbit antiserum (anti-UL35) was diluted 1:5,000 in PBS–0.1% Tween 20 containing 1% skim milk powder, whereas hybridoma supernatants (69-66 and 41-18) were used undiluted. After the filters were washed three times for 10 min in PBS–0.1% Tween 20 containing 1% skim milk powder, they were incubated for 1 h with horseradish peroxidase-conjugated secondary anti-mouse or anti-rabbit antibodies (DAKO) diluted 1:5,000 in PBS–0.1% Tween 20 containing 1% skim milk powder. Finally, the filters were washed two times for 10 min in PBS–0.1% Tween 20 containing 1% skim milk powder and for 10 min in PBS–0.1% Tween 20. Bound antibodies were detected using the ECL Western blotting detection reagents (Amersham Biosciences) according to the instructions of the manufacturer.

Immunofluorescence. For indirect immunofluorescence analysis, HFF were seeded onto glass coverslips in 24-well plates at 4×10^4 cells per well the day before infection. Cells were infected at an MOI of 0.2. For fixation, the cells were washed three times with PBS, incubated in 4% paraformaldehyde for 10 min, and washed four times with PBS. To permeabilize the cells, the coverslips were treated with PBS–0.2% Triton X-100 for 2 min and finally rinsed in PBS. To block nonspecific binding, the coverslips were first incubated in 10% normal horse serum for 20 min at 37°C. Subsequently, murine monoclonal antibodies directed against ppUL69 (antibody 69-66), ppUL82 (pp71) (antibody CMV355), ppUL83 (pp65) (antibody 28–77), ppUL99 (pp28) (antibody 41-18), or gpUL55 (gB) (antibody 27–287) were added as undiluted cell culture supernatants and incubated at 4°C for 2 h. After being washed three times for 5 min with PBS, the coverslips were incubated at 4°C for 2 h with anti-mouse goat serum labeled with fluorescein isothiocyanate as a secondary antibody (DAKO), which was used at a 1:50 dilution. In some experiments, cell nuclei were stained with DAPI (4′,6′-diamidino-2-phenylindole; 1 μg/ml). After two final washing steps in PBS, the coverslips were mounted on slides with Vectashield H-1000 (Vector, Burlingame, Calif.). Images were taken on an Axioscop 2 (Zeiss, Jena, Germany) fluorescence microscope.

Electron microscopy. For electron microscopy, cells were fixed with 2.5% glutaraldehyde and 1% sucrose in 0.1 M cacodylate buffer at pH 7.4. After postfixation in 2% osmium tetroxide, they were block stained in 2% uranyl acetate, dehydrated in a graded propanol series, and embedded in Epon (Fluka). Sections were cut parallel to the substrate to a thickness of 60 nm and contrast stained with uranyl acetate and lead citrate. Images were taken with a model 400 transmission electron microscope (Philips, Eindhoven, Netherlands) at an acceleration voltage of 80 kV.

RESULTS

Generation of a deletion mutant of UL35. To address the in vivo role of UL35, we first deleted the UL35 open reading frame in the viral genome, by using the HCMV AD169 genome as a BAC in *E. coli* (Fig. 1A). This deletion was achieved by RecET-based marker transfer in which we first exchanged the UL35 open reading frame with a kanamycin resistance gene. In a second step, the kanamycin gene was deleted by FLP-mediated recombination of two FRT sites flanking the resistance marker. The UL35 open reading frame was effectively removed from its start codon to its stop codon, thus deleting the coding sequences for both UL35 isoforms (24). The resulting BAC was named *del*UL35-BAC. Sequencing showed that an insertion of 80 bp remained as a mark from the recombination procedure. This insertion contained a single FRT site (34 bp) flanked by the two primer binding sites (each 23 bp) that were used for amplification of the kanamycin resistance cassette. An additional EcoRI restriction site was part of one primer binding site. In a similar way, a revertant virus was generated by reinserting the UL35 gene along with the kanamycin resistance marker into *del*UL35-BAC. Finally, the kanamycin gene was again removed by FLP-mediated recombination. This step resulted in a revertant BAC (*rev*UL35-BAC) with a single FRT site and an EcoRI restriction site remaining at the 3′ end of the UL35 open reading frame. The genomic organization and purity of all BACs were confirmed by PCR (data not shown), EcoRI restriction digestion, and Southern blot analysis, probing for UL35 and regions upstream and downstream of the deletion (Fig. 1B).

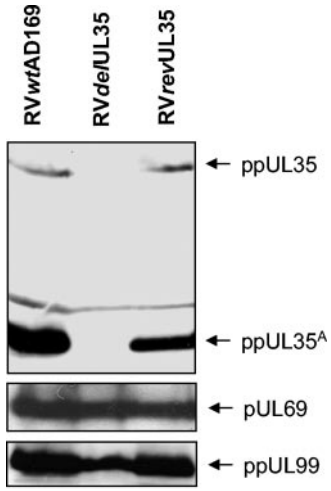

FIG. 2. Analysis of protein expression of cells infected with recombinant viruses. HFF were infected with RV*wt*AD169, RV*del*UL35, or RV*rev*UL35 (MOI, 0.1) and harvested at 96 hpi. Protein extracts were separated by SDS-polyacrylamide gel electrophoresis (SDS-PAGE) and transferred to a polyvinylidene difluoride membrane for immunoblot analysis. UL35 gene products were detected by an anti-UL35 rabbit antiserum. The two protein isoforms ppUL35 and ppUL35^A are indicated by arrows. After being stripped, the same blot was incubated with monoclonal antibodies directed against pUL69 or ppUL99 as controls.

Thereafter, the wild-type AD169-BAC, *del*UL35-BAC, and revertant *rev*UL35-BAC were electroporated into HFF to recover the recombinant viruses RV*wt*AD169, RV*del*UL35, and RV*rev*UL35, respectively. All viruses grew without the use of complementing cells, indicating that the UL35 gene is not an essential gene. However, recovery of RV*del*UL35 took about 3 weeks longer than did the wild-type or revertant virus, indicating a growth defect. Using lysates from infected cells in immunoblotting experiments, we could confirm that RV*del*UL35 did not show expression of both UL35 isoforms, ppUL35 and ppUL35A, whereas both proteins could be clearly detected in cells infected with wild-type (RV*wt*AD169) or revertant (RV*rev*UL35) viruses (Fig. 2). In contrast, the expression of two structural proteins, ppUL69 and ppUL99, did not show any significant difference in cells infected with the mutant virus RV*del*UL35.

As mentioned above, we had noticed a delay in virus replication after reconstitution of the RV*del*UL35. In order to investigate this delay in more detail, we compared the growth kinetics of all viruses at different MOIs. At an MOI of 0.1

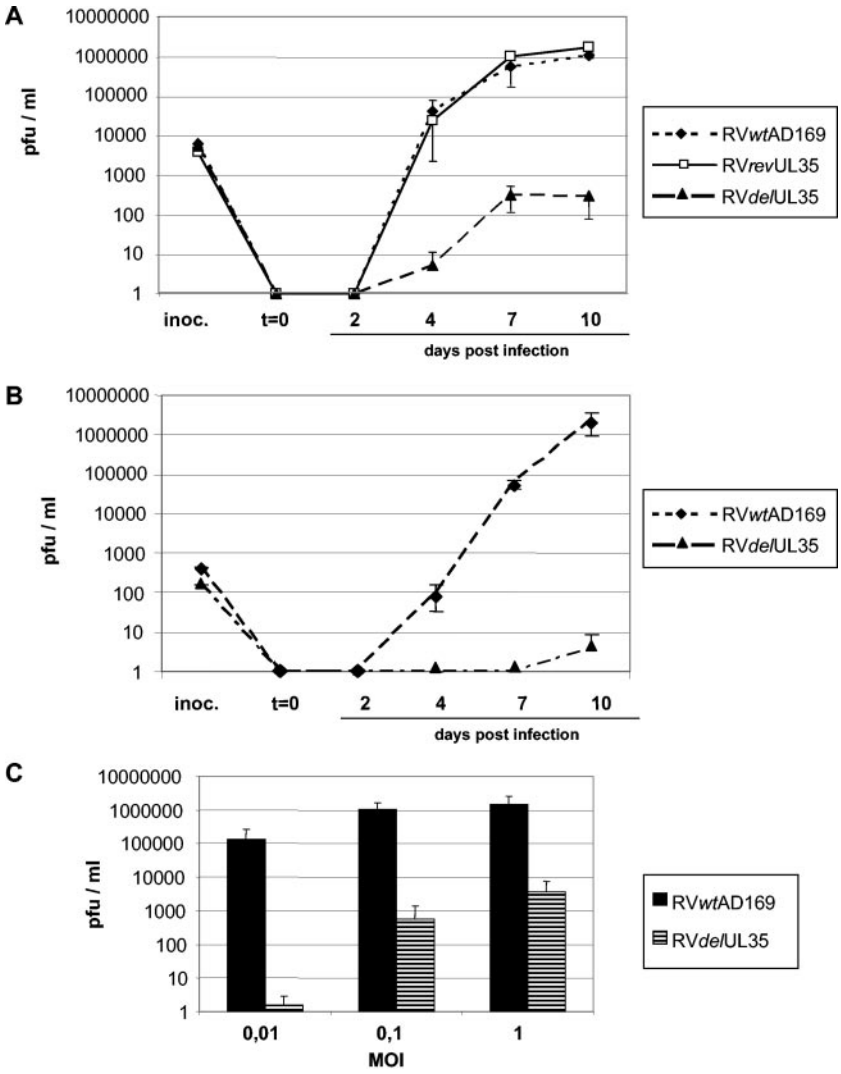

FIG. 3. Growth kinetics of recombinant viruses. (A) HFF were infected with RV*wt*AD169, RV*del*UL35, or RV*rev*UL35 at an MOI of 0.1. Cell culture supernatants were harvested at the indicated times after infection, and infectious virus was quantified by a plaque assay on HFF. The titer of the inoculum was determined in parallel (inoc.). (B) HFF were infected with RV*wt*AD169 or RV*del*UL35 at an MOI of 0.01. Virus yield was quantified as described for panel A. (C) HFF were infected in parallel with RV*wt*AD169 and RV*del*UL35 at MOIs of 0.01, 0.1, and 1. Cell culture supernatants were harvested at 10 dpi, and infectious virus was quantified by a plaque assay on HFF. Error bars indicate standard deviations.

PFU/cell, RV*del*UL35 replicated to titers more that 1,000-fold lower than those of the wild-type or revertant viruses (Fig. 3A). Wild-type and mutant viruses showed similar kinetics and reached a plateau in replication at about 7 days postinfection (dpi). However, at an MOI of 0.01 PFU/cell, the growth defect of the mutant virus RV*del*UL35 was much more apparent, as we did not observe a considerable production of infectious virus (Fig. 3B). Since several mutants of HCMV that show MOI-dependent growth have been described, we also compared the yields of wild-type and RV*del*UL35 viruses at 10 dpi after infection with different MOIs. Wild-type HCMV (RV*wt*AD169) showed a gradual rise in viral yield when a higher MOI was used (Fig. 3C). For the mutant RV*del*UL35, a comparable rise could only be seen at the higher MOIs of 0.1 and 1, but there was a drastic drop when an MOI of 0.01 was used. Interestingly, the mutant virus did not reach yields equivalent to those of the wild-type virus, even when infections were performed with an MOI of 1 PFU/cell. Thus, the mutant virus shows an MOI-dependent growth.

Uptake of viral DNA is unaffected in RV*del*UL35. Since a role for pUL35 in the activation of IE gene expression has been described previously (24, 38), we wanted to investigate the effect of the deletion of UL35 on the IE phase. For this, we first analyzed whether the uptake of regulatory virion proteins was comparable between wild-type and mutant viruses. HFF were infected with the wild-type and the UL35 deletion virus at the same MOI and analyzed for localization of the tegument proteins ppUL82 and ppUL69 at 4 hpi by immunofluorescence. As shown in Fig. 4A, both viruses showed similar uptakes of the tegument proteins ppUL82 and pUL69, indicating a normal entry of viral particles into cells.

Next, we investigated the uptake at the DNA level. For this, we first characterized the relative amount of viral DNA per PFU by serial dilutions of the inoculum followed by a PCR

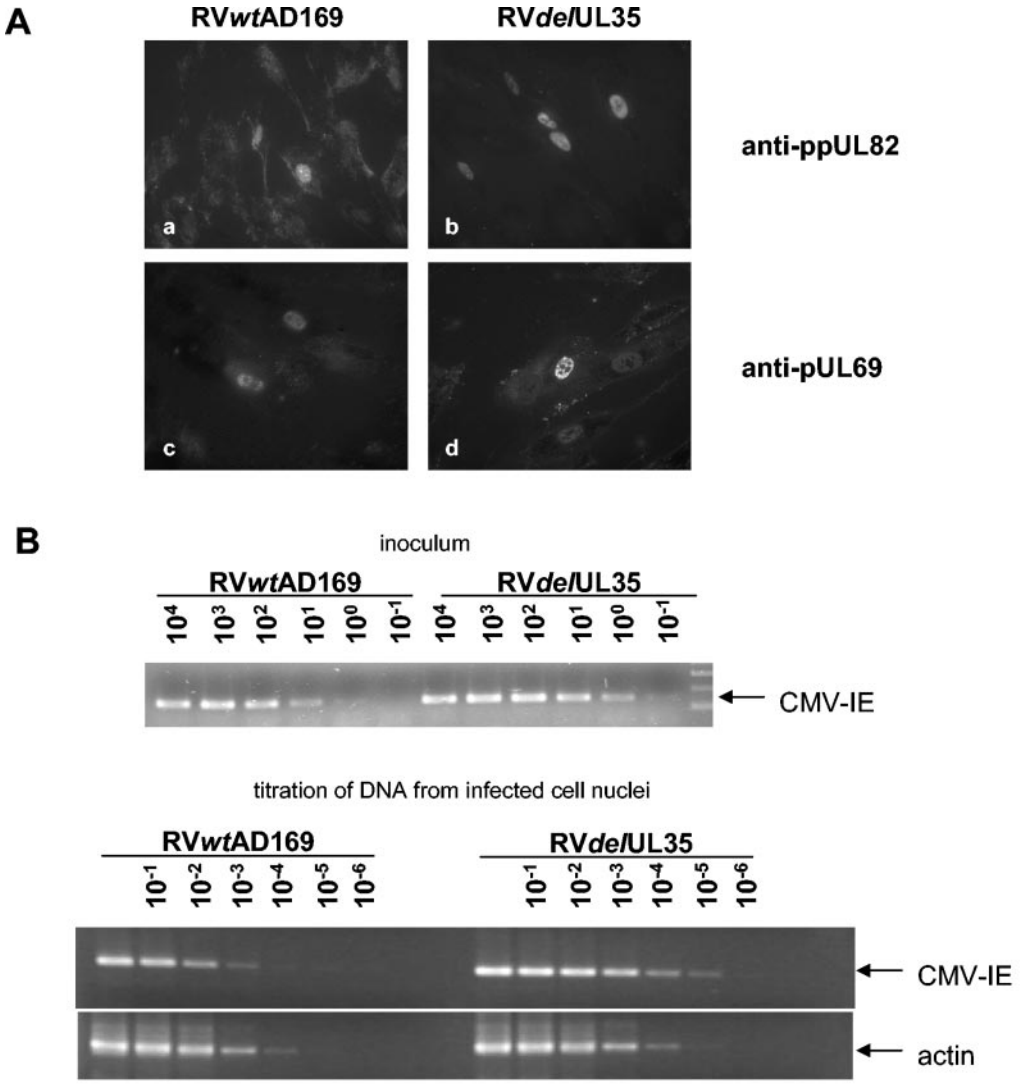

FIG. 4. Uptake of virus into cells. (A) Virus uptake into target cells was analyzed at the protein level by immunofluorescence. HFF were infected with RV*wt*AD169 or RV*del*UL35 at an MOI of 0.1. At 4 hpi, cells were stained with monoclonal antibodies recognizing tegument protein ppUL82 or pUL69. (B) Virus uptake was analyzed at the DNA level. Viral DNA present in the inoculum of infection was determined after DNA isolation and PCR titration in a 10-fold dilution series (upper panel). HFF were infected with RV*wt*AD169 or RV*del*UL35 at an MOI of 0.1. Cells were harvested at 6 hpi, and DNA was isolated from the nuclei of infected cells. The DNAs were titrated in a 10-fold dilution series and subjected to PCR to detect viral (HCMV IE region) or cellular (actin) DNA (lower panels).

specific for IE genes. For virus preparations that had been normalized for equal infectivities, we consistently observed approximately 10-fold more viral DNA per PFU for the mutant virus (Fig. 4B, upper panel). We then infected HFF with an MOI of 0.1 PFU/cell for both wild-type and mutant viruses. At 6 hpi, cells were harvested and the amounts of viral and cellular DNA were determined by PCR titration (Fig. 4B, lower panels). Consistent with the inoculum results, approximately 10-fold more viral DNA was recovered from cells infected with mutant virus. In contrast, similar levels were detected for the cellular actin gene that was used as a control. Therefore, we conclude that uptake of virus particles was not affected by deletion of UL35, but the viral DNA amount of RV*del*UL35 was about 10-fold higher than that of the wild-type virus when cells were infected at the same MOI.

Effect of UL35 deletion on IE gene expression. So far, all experiments were performed using MOIs as determined by a plaque assay. Plaques were counted after infected cells were stained for IE proteins. Thus, an effect of ppUL35 on the initiation of IE gene expression would be obscured by this outcome-based method of inoculum standardization. Our finding that the mutant virus inoculum contained a much larger amount of viral DNA per PFU than did the wild type (Fig. 4B, upper panel) supported the idea that more infectious particles of the mutant virus were needed to start a productive infection. Therefore, to investigate an effect on the IE phase, we decided to standardize the inoculum by determination of the amount of viral DNA in order have a physical measure of infectious particles. We used PCR titration to standardize the inoculum to similar amounts of

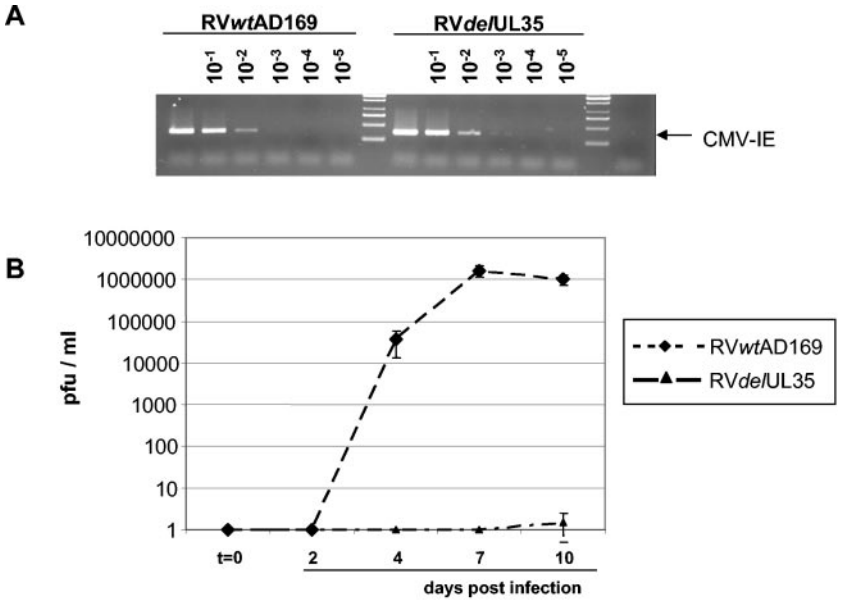

FIG. 5. Growth kinetics of recombinant viruses after standardization for genome equivalents. HFF were infected with wild-type (RV*wt*AD169) or mutant (RV*del*UL35) virus. (A) Inoculum of RV*del*UL35 was standardized on the basis of genome equivalents to an MOI of 0.1 of wild-type virus. Viral DNA was isolated from standardized inoculum, titrated in a 10-fold dilution series, and subjected to PCR to detect viral (HCMV IE region) DNA. (B) Cell culture supernatants were harvested at the indicated times after infection, and infectious virus was quantified by a plaque assay of HFF.

DNA for both wild-type and mutant viruses (Fig. 5A, 6A, and 7A).

First, we compared the growth levels of wild-type and mutant viruses that had been standardized for equal DNA contents. As can be seen in Fig. 5B, this standardization led to a more drastic difference in virus yields, with only little mutant virus being produced even 10 dpi. When we analyzed viral gene expression, we observed a significant reduction of IE gene expression in cells that were infected with the mutant virus (Fig. 6B). In cells infected with wild-type virus, a strong expression of IE proteins was visible at 24 hpi, while for the mutant virus at the same time only faint bands could be detected. In addition, expression of early and late proteins was hardly detectable. As a result, accumulation of viral DNA was also decreased (Fig. 7B and C, lanes 1 to 8). Therefore, we conclude that deletion of UL35 affects IE gene expression.

Effects of deletion of UL35 on virus assembly. For the investigation of a potential defect during the late phase, we used infection at the same MOI. Under these conditions, there should be no differences in IE gene expression and subsequent expression of other viral genes. To investigate whether this is the case, we characterized viral gene expression after infection of HFF with wild-type and mutant viruses at an MOI of 0.1 PFU/cell. At the indicated time points, cell extracts were prepared and used for immunoblotting to detect viral proteins representative for IE (IE1 and IE2), early (pUL44), and late (ppUL99) phases. As shown in Fig. 6C, both viruses showed similar expression kinetics for all viral proteins.

In addition, we addressed the influence of the deletion of UL35 on the genome replication kinetics of wild-type and mutant viruses. HFF were infected at an MOI of 0.1 and harvested at the indicated time intervals, and viral DNA accumulation was determined by Southern blot analysis. As shown in Fig. 7B and C (lanes 5 to 12), the DNA accumulations of both viruses (RV*wt*AD169 and RV*del*UL35) showed similar kinetics. Thus, the strongly reduced virus yield of RV*del*UL35 compared to that of the wild type after infection at equal MOIs is very likely not due to differences in viral DNA accumulation.

This result raised the possibility that the reduced accumulation of infectious virus in the supernatant of cells infected with mutant virus might result from impaired virus assembly. Therefore, we studied the ultrastructural aspects of particle maturation by the use of HFF infected with wild-type (Fig. 8A) or mutant (Fig. 8B) viruses at an MOI of 1. Infection was stopped at 72 hpi, and cells were prepared for electron microscopy. Analysis of the nuclei of infected cells showed that all three types of capsids, A (empty), B (with scaffold), or C (mature, DNA containing), were present. The quantitation of capsids from at least five sections gave similar proportions of all three capsid types in both wild-type and mutant infected cells. A clear difference was the electron-dense accumulations in the nuclei of RV*del*UL35-infected cells (Fig. 8C), which appeared to be free of capsids apart from some capsids at their boundaries. Another striking difference was observed after analysis of cytoplasmic sections. In cells infected with mutant virus, almost no dense bodies were found (Fig. 8B). Nevertheless, enveloped particles were present both in cells infected with wild-type or mutant virus. Cross sections of enveloped particles revealed no differences (Fig. 8D and E). When enveloped and nonenveloped particles were counted, the number of enveloped particles appeared to be reduced about 10-fold in cells infected with mutant virus.

As the formation of virions and dense bodies in the cytoplasm requires a correct localization of tegument and envelope proteins (20, 28, 37), we studied the localization of ppUL83 (pp65), ppUL82 (pp71), ppUL99 (pp28), and gpUL55 (gB) by immuno-

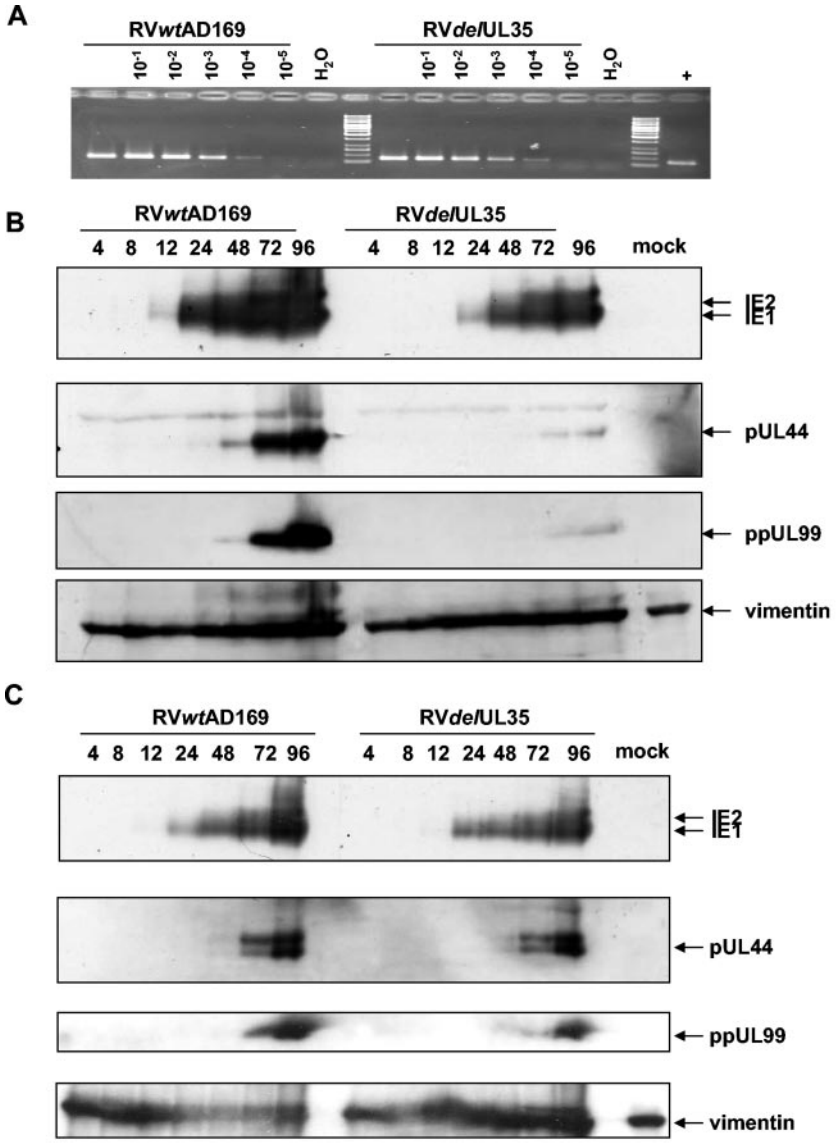

FIG. 6. Analysis of antigen expression in infected HFF. (A and B) HFF were infected with RV*wt*AD169 and RV*del*UL35 standardized for the same number of genome equivalents. (A) Standardization was controlled by PCR. Inoculum of RV*wt*AD169 was used at an MOI of 0.1. The inoculum of RV*del*UL35 was diluted to the same number of genome equivalents as that of RV*wt*AD169. Viral DNA was isolated from standardized inoculum, diluted in a 10-fold dilution series, and subjected to PCR to detect viral (HCMV IE region) DNA. (B) Cell lysates from HFF infected with standardized inoculum of RV*wt*AD169 or RV*del*UL35 were prepared at the indicated time points and separated by SDS-PAGE. Representative HCMV IE (IE1 and IE2), early (pUL44), and late (ppUL99) proteins were detected with monoclonal antibodies E13, CCH2, and 41-18, respectively. The cellular protein vimentin was stained with monoclonal antibody Ab-1 as a loading control. (C) HFF were infected with RV*wt*AD169 or RV*del*UL35 at an MOI of 0.1. Cells lysates were prepared at the indicated time points and separated by SDS-PAGE. The same antibodies as those described for panel B were used for detection.

fluorescence analysis after infection at the same MOIs. No difference was observed when ppUL99 (pp28) and gpUL55 (gB) were analyzed, as both proteins accumulated at a cytoplasmic location close to the *trans*-Golgi network (Fig. 9, panels 2e to 2h and 3e to 3h). Staining of ppUL82 and ppUL83 revealed a nuclear localization of both proteins in cells infected with wild-type or mutant virus (Fig. 9, panels 1a to 1d). In cells infected with wild-type virus, however, both proteins translocated to the cytoplasm during the later stages of infection (Fig. 9, panels 2a, 2c, 3a, and 3c). In contrast, in cells infected with mutant virus RV*del*UL35, both proteins remained in the nucleus up to 120 hpi (Fig. 9, panels 2b, 2d, 3b, and 3d), the latest time point analyzed. This finding in conjunction with the observed decrease of enveloped particles in cells infected with the mutant virus suggests that late events during assembly are impaired in the mutant virus, thus leading to a reduced release of infectious particles.

DISCUSSION

The MIEP is a central control unit that processes cellular and viral signals to make a decision between latent or lytic infection of HCMV (26, 31, 32). Among the viral signals, the

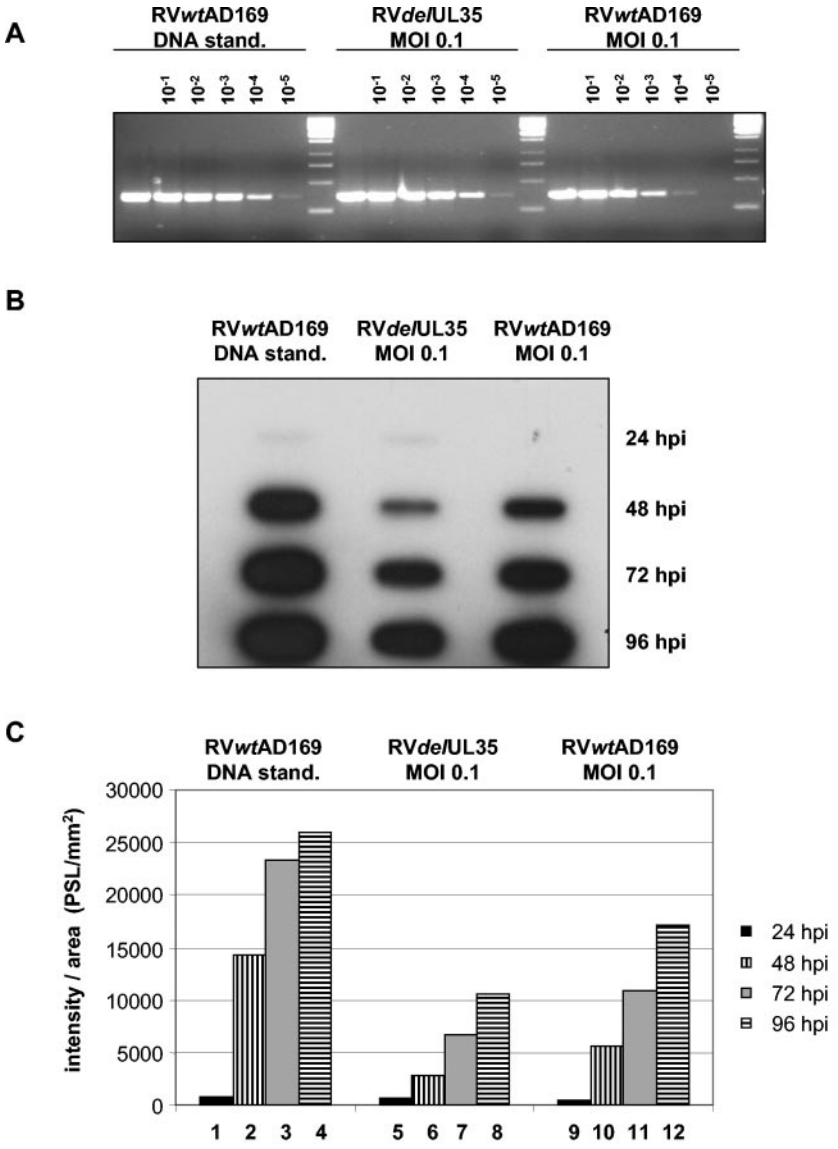

FIG. 7. DNA accumulation in infected cells. (A) PCR titration of the inoculum used for infection of HFF. An inoculum of RV*del*UL35 or RV*wt*AD169 was used for infection of HFF at an MOI of 0.1. In addition, an inoculum of RV*wt*AD169 was standardized to RV*del*UL35 (MOI, 0.1) for equal amounts of viral DNA (DNA stand.). Viral DNA was isolated from inocula of all three samples, diluted in a 10-fold dilution series, and subjected to PCR to detect viral (HCMV IE region) DNA. (B) HFF were infected with the inoculum characterized for panel A. Equal amounts of cells were harvested at the indicated time points and used for DNA isolation. Isolated DNAs were slot blotted onto a nitrocellulose membrane and hybridized with a radioactively labeled probe directed against UL36. (C) Radioactivity bound to the filter shown in panel B was quantified by phosphorimager analysis.

tegument proteins ppUL82 and ppUL35 have been shown to interact physically and to transactivate the MIEP alone and cooperatively (24, 38). We wanted to analyze the biological role of UL35 proteins by generating a virus mutant with deletion of the UL35 gene. One-step growth curves showed that virus production was decreased 1,000-fold when cells were infected with the mutant virus at an MOI of 0.1. This defect could be reversed when the UL35 gene was reinserted. This observation makes the deletion of UL35 the sole reason for the growth defect.

Our observation of reduced virus production by the UL35 deletion virus is supported by a recent large-scale analysis in which a similar deletion of UL35 was generated (13). In addition, our deletion of UL35 in the genetic background of a clinical isolate showed a comparably reduced virus yield (M. Winkler and K. Schierling, unpublished data). However, in a second large-scale analysis, UL35 was classified as nonessential, with yields reduced less than 10-fold (49). This discrepancy is likely explained by the different targeting strategies, since in the second approach a transposon insertion into the amino-terminal region was created. Since the UL35 gene encodes two coterminal protein species (24), the transposon insertion targeted only the full-length ppUL35, leaving the short-form ppUL35A intact. Therefore, either ppUL35A was able to compensate for ppUL35 or the essential part resides in the C

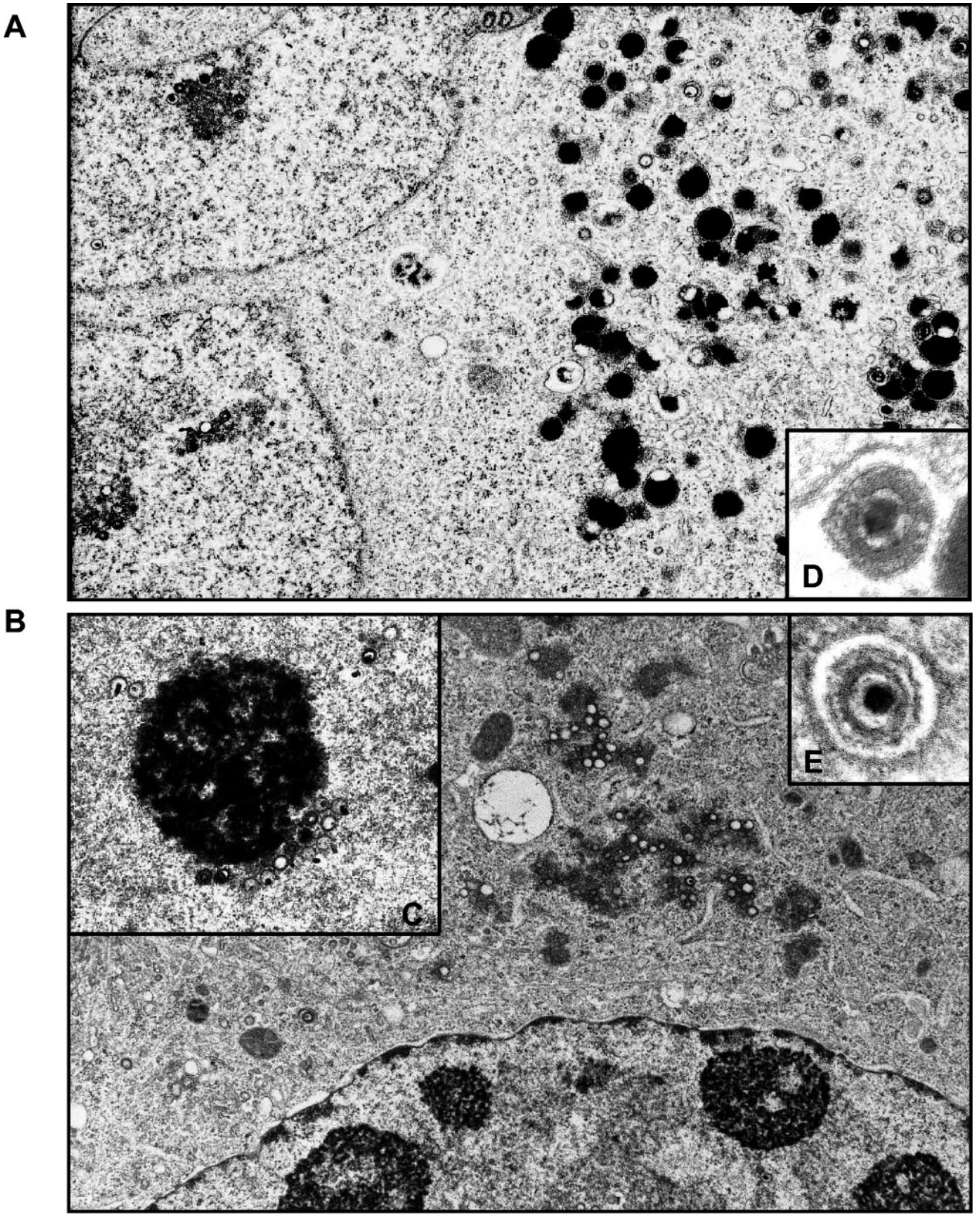

FIG. 8. Ultrastructural analysis of virus maturation. HFF cells were infected with RV*wt*AD169 or RV*del*UL35 at an MOI of 1. Cells were fixed at 72 hpi and processed for electron microscopy. Overview images of cells infected with RV*wt*AD169 (A) or RV*del*UL35 (B) were taken at ×8,000 magnification. (C) Detail of nuclear electron-dense structures in cells infected with the mutant at ×20,000 magnification. (D and E) Representative images of virions of RV*wt*AD169 and RV*del*UL35, respectively, taken at ×80,000 magnification.

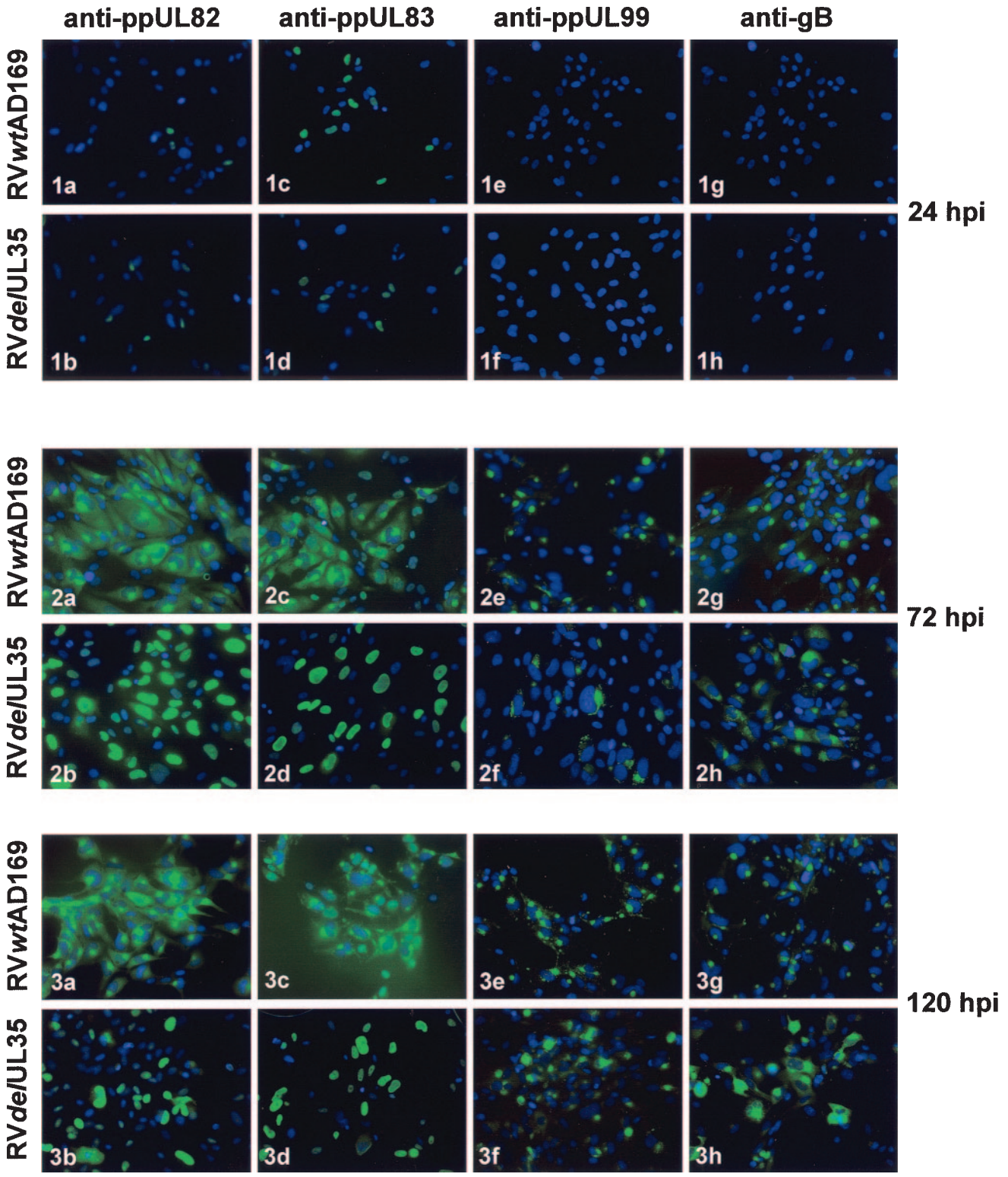

FIG. 9. Immunofluorescence analysis of virus maturation. HFF were infected with RV*wt*AD169 or RV*del*UL35 at an MOI of 0.2. Cells were fixed at indicated time points (24, 72, and 120 hpi) and stained with monoclonal antibodies directed against ppUL82 (CMV355), ppUL83 (28–77), ppUL99 (41-18), and gpUL55 (27–287), as indicated at the top. Goat anti-mouse secondary antibody labeled with fluorescein isothiocyanate was used for detection. The nuclei were stained with DAPI. See the text for details.

termini of the UL35 proteins. The latter possibility is supported by the observation that the addition of a hemagglutinin tag at the end of the UL35 gene in the context of the viral genome leads to a reduction in viral yield similar to that resulting from the deletion of UL35 (Schierling and Winkler, unpublished data).

It was reported previously that ppUL35 has a role in the transactivation of the MIEP and efficient initiation of IE phase (24, 38). The MOI dependence of the RV*del*UL35 virus yield is compatible with this view, since mutations in other genes implicated in IE regulation and gene expression, such as the ppUL82, ppUL69, ppUL123 (IE1) genes, and enhancer deletions showed similar behaviors (6, 15, 19, 25, 29). In addition, when infection was done at an MOI determined by plaque titration with an anti-IE antibody, we observed that the DNA amount in that inoculum of the RV*del*UL35 mutant was 10-fold higher than that in the wild-type virus. As the particles appeared to be normal when analyzed by electron microscopy, this observation would mean that a 10-fold-higher number of particles of the mutant virus was required to reach the same infectivity as that of the wild-type virus. Thus, the lack of ppUL35 would be compensated by a higher amount of input viral DNA, by higher levels of other tegument proteins, or by a combination of both. When we standardized our inoculum to equal amounts of input DNA, we observed a delayed IE gene expression and consequently a strongly reduced expression of early and late proteins. This resulted in a significant reduction of viral DNA accumulation and a strongly reduced virus yield. In agreement with an effect on IE gene expression, an MOI-dependent virus yield was observed, rendering UL35 an essential gene when cells were infected at the low MOI of 0.01.

Defects in IE gene expression can be compensated by a high input of viral particles, which has been observed previously in conjunction with an HCMV mutant carrying a deletion in the distal enhancer (25). A possible explanation for the decreased IE gene expression with the mutant RV*del*UL35 could be that no ppUL82 was packaged into viral particles, since during late phase there was no translocation of ppUL82 towards the cytoplasm. Due to the low yields of the RV*del*UL35 mutant, we were not able to address this point experimentally. When we analyzed the uptake of tegument proteins into cells infected with wild-type or mutant virus, we observed similar numbers of cells staining positive for ppUL82 or ppUL69. Therefore, the defect in IE gene expression should be due mainly to a lack of ppUL35 and a subsequent failure of sufficient cooperative activation of the MIEP.

When infections were carried out using the same MOI for both wild-type and mutant viruses, we observed no difference in viral protein expression. Additionally, the accumulations of viral DNA showed comparable levels and kinetics after infection with wild-type or mutant viruses. As ppUL35 apparently had no influence on early or late gene expression or viral DNA replication, we could use infections standardized to the same MOI to investigate an effect of UL35 during the late phase.

Hereby, we observed an altered virus maturation in cells infected with mutant virus. This alteration was most clearly indicated by the absence of dense bodies. In addition, quantitation of cytoplasmic virus particles showed 10-fold fewer mature enveloped particles when cells were infected with mutant virus. The lack of dense bodies could be explained by the retention of ppUL83 (pp65) in the nucleus, as a virus mutant lacking the UL83 gene also failed to produce dense bodies (39). It is believed that dense bodies accumulate during high-titer passage of HCMV. Therefore, the mutant virus, which produces much lower titers, should be less prone to accumulate dense bodies. However, our reconstituted wild-type virus had the same passage history, and it was the mutant virus for which the higher titers had to be employed for virus stock production. In addition, immunofluorescence staining of cells demonstrated that several viral proteins (ppUL99 and gpUL55) showed normal accumulations and distributions in the cytoplasm of infected cells. It is therefore likely that the failure to produce dense bodies reflects a specific defect in the envelopement of viral particles.

In the nucleus, large accumulations of electron-dense material were observed. At present, the nature of these structures is unclear. Electron density in the nucleus usually corresponds to DNA, indicating that these structures could represent domains of condensed viral genomes. As viral particles can be seen at the margin of this material, a possible reason for this accumulation could be a packaging defect. However, we observed similar ratios of viral capsid types in the nuclei of cells infected with wild-type and mutant viruses, making a packaging problem unlikely. Therefore, these structures require further investigation.

At present, it is unclear how ppUL35 could be responsible for the translocation of ppUL82 and ppUL83 (pp65) from the nucleus to the cytoplasm. A similar phenotype has been described for a mutant of HCMV with a lack of TRS1 (5), and a recently published analysis of this mutant argued that pTRS1 has a role in the encapsidation of viral DNA since the number of C capsids was reduced (1). In our electron microscopic analysis, we did not detect such a difference. In contrast, the lack of dense bodies and the reduced amount of enveloped particles argue for a role of ppUL35 in the cytoplasmic particle assembly. As UL35 proteins interact with ppUL82 but not with ppUL83 (38), their effect on tegument protein localization might be independent of physical interaction. We therefore favor the hypothesis that ppUL35 of ppUL35A might directly or indirectly influence nucleocytoplasmic transport pathways, either enhancing export of tegument proteins from the nucleus or blocking import of tegument proteins into the nucleus during the late phase.

In summary, we could show that ppUL35 plays an important role in both IE gene expression and virus assembly. Further studies will be required to elucidate the underlying mechanisms and to address the question of whether the effects on IE gene expression and virus maturation are direct or indirect.

ACKNOWLEDGMENTS

We thank A. Lüske for technical assistance and H. Hofmann for critical discussion. We also thank U. Koszinowski and M. Wagner for plasmids pSL-FRT, pKD46, pBRep-cre, and HCMV AD169-BAC(pHB15) and T. Stamminger, M. Mach, and B. Biegalke for murine monoclonal antibodies CMV355, 41-18, 28–77, and 27–287 and rabbit antiserum against pUL35.

This work was supported by grants from the Deutsche Forschungsgemeinschaft (Wi 1725/2-1), the IZKF Ulm (H4, 01KS9605/2), and the Universität Ulm (P.680) to M. Winkler.

REFERENCES

1. **Adamo, J. E., J. Schroer, and T. Shenk.** 2004. Human cytomegalovirus TRS1 protein is required for efficient assembly of DNA-containing capsids. J. Virol. **78:**10221–10229.
2. **Atalay, R., A. Zimmermann, M. Wagner, E. Borst, C. Benz, M. Messerle, and H. Hengel.** 2002. Identification and expression of human cytomegalovirus transcription units coding for two distinct Fcγ receptor homologs. J. Virol. **76:**8596–8608.
3. **Baxter, M. K., and W. Gibson.** 2001. Cytomegalovirus basic phosphoprotein (pUL32) binds to capsids in vitro through its amino one-third. J. Virol. **75:**6865–6873.
4. **Bechtel, J. T., and T. Shenk.** 2002. Human cytomegalovirus UL47 tegument protein functions after entry and before immediate-early gene expression. J. Virol. **76:**1043–1050.
5. **Blankenship, C. A., and T. Shenk.** 2002. Mutant human cytomegalovirus lacking the immediate-early TRS1 coding region exhibits a late defect. J. Virol. **76:**12290–12299.
6. **Bresnahan, W. A., and T. E. Shenk.** 2000. UL82 virion protein activates expression of immediate early viral genes in human cytomegalovirus-infected cells. Proc. Natl. Acad. Sci. USA **97:**14506–14511.
7. **Britt, W. J., and L. Vugler.** 1987. Structural and immunological characterization of the intracellular forms of an abundant 68,000 Mr human cytomegalovirus protein. J. Gen. Virol. **68:**1897–1907.
8. **Browne, E. P., and T. Shenk.** 2003. Human cytomegalovirus UL83-coded pp65 virion protein inhibits antiviral gene expression in infected cells. Proc. Natl. Acad. Sci. USA **100:**11439–11444.
9. **Cherepanov, P. P., and W. Wackernagel.** 1995. Gene disruption in Escherichia coli: Tc^R and Km^R cassettes with the option of Flp-catalyzed excision of the antibiotic-resistance determinant. Gene **158:**9–14.
10. **Child, S. J., M. Hakki, K. L. De Niro, and A. P. Geballe.** 2004. Evasion of cellular antiviral responses by human cytomegalovirus *TRS1* and *IRS1*. J. Virol. **78:**197–205.
11. **Datsenko, K. A., and B. L. Wanner.** 2000. One-step inactivation of chromosomal genes in *Escherichia coli* K-12 using PCR products. Proc. Natl. Acad. Sci. USA **97:**6640–6645.
12. **Davison, A. J., A. Dolan, P. Akter, C. Addison, D. J. Dargen, D. J. Alcendor, D. J. McGeoch, and G. S. Hayward.** 2003. The human cytomegalovirus genome revisited: comparison with the chimpanzee cytomegalovirus genome. J. Gen. Virol. **84:**17–28.
13. **Dunn, W., C. Chou, H. Li, R. Hai, D. Patterson, V. Stolc, H. Zhu, and F. Liu.** 2003. Functional profiling of a human cytomegalovirus genome. Proc. Natl. Acad. Sci. USA **100:**14223–14228.
14. **Gawn, J. M., and R. F. Greaves.** 2002. Absence of IE1 p72 protein function during low-multiplicity infection by human cytomegalovirus results in a broad block to viral delayed-early gene expression. J. Virol. **76:**4441–4455.
15. **Ghazal, P., M. Messerle, K. Osborn, and A. Angulo.** 2003. An essential role of the enhancer for murine cytomegalovirus in vivo growth and pathogenesis. J. Virol. **77:**3217–3228.
16. **Gibson, W.** 1996. Structure and assembly of the virion. Intervirology **39:**389–400.
17. **Gilbert, M. J., S. R. Riddell, B. Plachter, and P. D. Greenberg.** 1996. Cytomegalovirus selectively blocks antigen processing and presentation of its immediate-early gene product. Nature **383:**720–722.
18. **Gu, H., Y. R. Zou, and K. Rajewsky.** 1993. Independent control of immunoglobulin switch recombination at individual switch regions evidenced through Cre-loxP-mediated gene targeting. Cell **73:**1155–1164.
19. **Hayashi, M. L., C. Blankenship, and T. Shenk.** 2000. Human cytomegalovirus UL69 protein is required for efficient accumulation of infected cells in the G1 phase of the cell cycle. Proc. Natl. Acad. Sci. USA **97:**2692–2696.
20. **Hensel, G., H. Meyer, S. Gartner, G. Brand, and H. F. Kern.** 1995. Nuclear localization of the human cytomegalovirus tegument protein pp150 (ppUL32). J. Gen. Virol. **76:**1591–1601.
21. **Hobom, U., W. Brune, M. Messerle, G. Hahn, and U. H. Koszinowski.** 2000. Fast screening procedures for random transposon libraries of clones herpesvirus genomes: mutational analysis of human cytomegalovirus envelope glycoprotein genes. J. Virol. **74:**7720–7729.
22. **Howell, C. L., and M. J. Miller.** 1983. Effect of sucrose phosphate and sorbitol on infectivity of enveloped viruses during storage. J. Clin. Microbiol. **18:**658–662.
23. **Liu, B., and M. F. Stinski.** 1992. Human cytomegalovirus contains a tegument protein that enhances transcription from promoters with upstream ATF and AP-1 *cis*-acting elements. J. Virol. **66:**4434–4444.
24. **Liu, Y., and B. J. Biegalke.** 2002. The human cytomegalovirus UL35 gene encodes two proteins with different functions. J. Virol. **76:**2460–2468.
25. **Meier, J. L., M. J. Keller, and J. J. McCoy.** 2002. Requirement of multiple *cis*-acting elements in the human cytomegalovirus major immediate-early distal enhancer for viral gene expression and replication. J. Virol. **76:**313–326.
26. **Meier, J. L., and M. F. Stinski.** 1996. Regulation of human cytomegalovirus immediate-early gene expression. Intervirology **39:**331–342.
27. **Mettenleiter, T. C.** 2002. Herpesvirus assembly and egress. J. Virol. **76:**1537–1547.
28. **Meyer, H. H., A. Ripalti, M. P. Landini, K. Radsak, H. F. Kern, and G. M. Hensel.** 1997. Human cytomegalovirus late-phase maturation is blocked by stably expressed UL32 antisense mRNA in astrocytoma cells. J. Gen. Virol. **78:**2621–2631.
29. **Mocarski, E. S., G. W. Kemble, J. M. Lyle, and R. F. Greaves.** 1996. A deletion mutant in the human cytomegalovirus gene encoding IE1(491aa) is replication defective due to a failure in autoregulation. Proc. Natl. Acad. Sci. USA **93:**11321–11326.
30. **Murphy, E., I. Rigoutsos, T. Shibuya, and T. E. Shenk.** 2003. Reevaluation of human cytomegalovirus coding potential. Proc. Natl. Acad. Sci. USA **100:**13585–13590.
31. **Murphy, J. C., W. Fischle, E. Verdin, and J. H. Sinclair.** 2002. Control of cytomegalovirus lytic gene expression by histone acetylation. EMBO J. **21:**1112–1120.
32. **Nelson, J. A., J. W. Gnann, Jr., and P. Ghazal.** 1990. Regulation and tissue-specific expression of human cytomegalovirus. Curr. Top. Microbiol. Immunol. **154:**75–100.
33. **Nowak, B., C. Sullivan, P. Sarnow, R. Thomas, F. Bricout, J. C. Nicolas, B. Fleckenstein, and A. J. Levine.** 1984. Characterization of monoclonal antibodies and polyclonal immune sera directed against human cytomegalovirus virion proteins. Virology **132:**325–338.
34. **Pass, R. F.** 2001. Cytomegalovirus, p. 2675–2705. *In* D. M. Knipe and P. M. Howley (ed.), Fields virology, vol. 2. Lippincott Williams & Wilkins, Philadelphia, Pa.
35. **Plachter, B., W. Britt, R. Vornhagen, T. Stamminger, and G. Jahn.** 1993. Analysis of proteins encoded by IE regions 1 and 2 of human cytomegalovirus using monoclonal antibodies generated against recombinant antigens. Virology **193:**642–652.
36. **Romanowski, M. J., and T. Shenk.** 1997. Characterization of the human cytomegalovirus *irs1* and *trs1* genes: a second immediate-early transcription unit within *irs1* whose product antagonizes transcriptional activation. J. Virol. **71:**1485–1496.
37. **Sanchez, V., K. D. Greis, E. Sztul, and W. J. Britt.** 2000. Accumulation of virion tegument and envelope proteins in a stable cytoplasmic compartment during human cytomegalovirus replication: characterization of a potential site of virus assembly. J. Virol. **74:**975–986.
38. **Schierling, K., T. Stamminger, T. Mertens, and M. Winkler.** 2004. Human cytomegalovirus tegument proteins ppUL82 (pp71) and ppUL35 interact and cooperatively activate the major immediate-early enhancer. J. Virol. **78:**9512–9523.
39. **Schmolke, S., H. F. Kern, P. Drescher, G. Jahn, and B. Plachter.** 1995. The dominant phosphoprotein pp65 (UL83) of human cytomegalovirus is dispensable for growth in cell culture. J. Virol. **69:**5959–5968.
40. **Silva, M. C., Q.-C. Yu, L. Enquist, and T. Shenk.** 2003. Human cytomegalovirus UL99-encoded pp28 is required for the cytoplasmic envelopment of tegument-associated capsids. J. Virol. **77:**10594–10605.
41. **Sinzger, C., M. Kahl, K. Laib, K. Klingel, P. Rieger, B. Plachter, and G. Jahn.** 2000. Tropism of human cytomegalovirus for endothelial cells is determined by a post-entry step dependent on efficient translocation to the nucleus. J. Gen. Virol. **81:**3021–3035.
42. **Sinzger, C., J. Knapp, K. Schmidt, M. Kahl, and G. Jahn.** 1999. A simple and rapid method for preparation of viral DNA from cell associated cytomegalovirus. J. Virol. Methods **81:**115–122.
43. **Varnum, S. M., D. N. Streblow, M. E. Monroe, P. Smith, K. J. Auberry, L. Pasa-Tolic, D. Wang, D. G. Camp, K. Rodland, S. Wiley, W. Britt, T. Shenk, R. D. Smith, and J. A. Nelson.** 2004. Identification of proteins in human cytomegalovirus (HCMV) particles: the HCMV proteome. J. Virol. **78:**10960–10966.
44. **Wagner, M., A. Gutermann, J. Podlech, M. J. Reddehase, and U. H. Koszinowski.** 2002. Major histocompatibility complex class I allele-specific cooperative and competitive interactions between immune evasion proteins of cytomegalovirus. J. Exp Med. **196:**805–816.
45. **Winkler, M., T. Aus dem Siepen, and T. Stamminger.** 2000. Functional interaction between pleiotropic transactivator pUL69 of human cytomegalovirus and the human homolog of yeast chromatin regulatory protein SPT6. J. Virol. **74:**8053–8064.
46. **Winkler, M., S. A. Rice, and T. Stamminger.** 1994. UL69 of human cytomegalovirus, an open reading frame with homology to ICP27 of herpes simplex virus, encodes a transactivator of gene expression. J. Virol. **68:**3943–3954.
47. **Winkler, M., S. Schmolke, B. Plachter, and T. Stamminger.** 1995. The pUL69 protein of human cytomegalovirus (HCMV), a homologue of the herpes simplex virus ICP27, is contained within the tegument of virions and activates the major immediate-early enhancer of HCMV in synergy with the tegument protein pp71 (ppUL82). Scand J. Infect. Dis. Suppl. **99:**8–9.
48. **Winkler, M., and T. Stamminger.** 1996. A specific subform of the human cytomegalovirus transactivator protein pUL69 is contained within the tegument of virus particles. J. Virol. **70:**8984–8987.
49. **Yu, D., M. C. Silva, and T. Shenk.** 2003. Functional map of human cytomegalovirus AD169 defined by global mutational analysis. Proc. Natl. Acad. Sci. USA **100:**12396–12401.